Unusual Transformation from Strong Negative to Positive Thermal Expansion in $PbTiO_3$-$BiFeO_3$ Perovskite

Jun Chen,[1,*] Longlong Fan,[1] Yang Ren,[2] Zhao Pan,[1] Jinxia Deng,[1] Ranbo Yu,[1] and Xianran Xing[1,3,†]

[1]*Department of Physical Chemistry, University of Science and Technology Beijing, Beijing 100083, China*

[2]*Argonne National Laboratory, X-Ray Science Division, Argonne, Illinois 60439, USA*

[3]*State Key Laboratory for Advanced Metals and Materials, University of Science and Technology Beijing, Beijing 100083, China*

(Received 26 September 2012; revised manuscript received 16 January 2013; published 14 March 2013)

Tetragonal $PbTiO_3$-$BiFeO_3$ exhibits a strong negative thermal expansion in the $PbTiO_3$-based ferroelectrics that consist of one branch in the family of negative thermal expansion materials. Its strong negative thermal expansion is much weakened, and then unusually transforms into positive thermal expansion as the particle size is slightly reduced. This transformation is a new phenomenon in the negative termal expansion materials. The detailed structure, temperature dependence of unit cell volume, and lattice dynamics of $PbTiO_3$-$BiFeO_3$ samples were studied by means of high-energy synchrotron powder diffraction and Raman spectroscopy. Such unusual transformation from strong negative to positive thermal expansion is highly associated with ferroelectricity weakening. An interesting zero thermal expansion is achieved in a wide temperature range (30–500 °C) by adjusting particle size due to the negative-to-positive transformation character. The present study provides a useful method to control the negative thermal expansion not only for ferroelectrics but also for those functional materials such as magnetics and superconductors.

DOI: 10.1103/PhysRevLett.110.115901 PACS numbers: 65.40.De, 61.05.cp, 77.80.B−

Negative thermal expansion (NTE) materials, whose volume abnormally contracts with heating, have been paid much attention in the past two decades [1–3]. The most promising advantage of the occurrence of NTE could be utilized to control the thermal expansion, in order to obtain a desirable coefficient of thermal expansion (CTE) of not only composites but also single phase materials [2,3]. The understanding on the mechanism of NTE is still the main challenge to find more NTE materials. The soft-phonon NTE mechanism has been well studied in those materials with open frame structure, such as ZrW_2O_8 and ScF_3 [1–4]. However, a large amount of NTE materials exhibit a strong coupling between NTE and physical properties such as magnetic ordering in Invar alloys [5], or change of valence state in $LaCu_3Fe_4O_{12}$ [6]. Interestingly, the NTE has been found in the family of perovskite-type ABO_3 ferroelectrics. The CTE of $PbTiO_3$ (PT) based materials can be well adjusted by suitable substitutions of different cations [7–11]. Furthermore, a colossal NTE was recently found in perovskite $BiNiO_3$, which is correlated to a change of valence state [12].

In order for NTE materials to be utilized in applications such as thin films or nanodevices, the effect of a decreasing dimension could be significant for the thermal expansion behavior. For example, NTE was found in Au nanoparticles over a wide temperature range, which was explained by the effects of a valence electron potential on equilibrium lattice separations [13]. Much enhanced NTE was found in the in-plane lattice parameter of graphene up to 900 K [14]. Also, giant NTE is a result of strong coupling between magnetism and crystal lattice for magnetic nanocrystals, such as CuO and MnF_2 [15]. The studies on the effect of small dimension on NTE will definitely bring more interesting results and contribute to the progress on the NTE design. According to the previous reports, the NTE are generally produced or enhanced by a decreasing dimension, such as Au nanoparticles, graphene, and magnetic nanocrystals [13–15]. However, transformation from negative to positive thermal expansion was never observed. In the present study, we report that a strong NTE is unusually transformed to positive thermal expansion (PTE) in the PT-based materials by reducing particle size. Interestingly a zero thermal expansion (ZTE) can be achieved due to such a character as negative-to-positive transformation. The thermal expansion properties and detailed structure were investigated by high-energy synchrotron powder diffraction (SPD) and Raman spectroscopy. The transformation of strong negative to positive thermal expansion is a result of weakened ferroelectricity. The present study gives a useful method to control the thermal expansion of multifunctional materials.

$0.7PbTiO_3$-$0.3BiFeO_3$ (PT-BF) samples were prepared by a sol-gel method. The single-phase sample with different particle size can be obtained by calcining gel at various temperatures. The samples were calcined at temperatures of 700 °C, 750 °C, 800 °C, and 900 °C for 3 h, respectively. High temperature synchrotron powder diffraction data were collected from room temperature (RT) to 600 °C at beam line 11-ID-C at the advanced photon source. The wavelength of synchrotron light was 0.10804 Å. The detailed structure was refined based on the full-profile Rietveld method performed on the software FULLPROF. The details

of the sample preparation, thermal analysis, microstructure, structural refinements, and dielectric properties are given in the Supplemental Material [16].

It has been known that the NTE of PT can be adjusted by chemical modification, which often comes with the caveat of weakening the NTE and reducing the Curie temperature (T_C) [7]. So far, only two PT-based systems have been found to exhibit an enhanced NTE upon chemical modification: (Pb, Cd)TiO_3 and PT-BF [10,11]. In general, PT-based NTE materials show a nonlinear volume contraction as function of temperature. The main contribution to the NTE occurs as the temperature approaches the T_C. However, there is a special composition of 0.7PT-0.3BF whose unit cell volume contracts almost linearly with increasing temperature [10]. Its NTE is linear and strong. Therefore, the composition of 0.7PT-0.3BF is adopted in the present study.

Dried gel powders of 0.7PT-0.3BF were calcined at different temperatures in order to control the particle size. A crystalline bulk sample can be obtained at a calcining temperature of 900 °C, which is confirmed by observation of the sharp SPD peaks (Fig. 1). However, with decreasing calcination temperature, a pronounced change appears. Not only do the SPD profiles become broader but also splitting between the diffraction peaks, such as (002) and (200), becomes less pronounced (Fig. 1), indicating that the crystal structure is greatly affected by the changes in the particle size. In order to make the following discussion convenient, the samples calcined at 900 °C, 800 °C, 750 °C, and 700 °C are labeled as S-I, S-II, S-III, and S-IV, respectively.

The particle size and morphology were examined by both high-resolution TEM (HRTEM) and field-emission SEM. The sample S-I has micron-scale particle sizes, while the samples S-II, S-III, and S-IV have much smaller sizes of 160 nm, 140 nm, and 110 nm, respectively, with a uniform morphology distribution [16]. Figure 2 represents the microstructure for the S-IV, obtained from TEM. It should be noted that the particle size observed by TEM agrees well with the calculation with full width at half maximum of x-ray diffraction and SEM investigations. The selected-area electron diffraction can be well indexed and agrees well with the SPD calculation. The HRTEM image on a typical individual nanocube confirms that the sample has a nature of single-crystalline structure [Fig. 2(b)]. The interplanar spaces of about 2.31 and 4.12 Å correspond to (111) and (001), respectively.

In order to achieve the detailed structure information, the structural parameters of diffraction pattern obtained from high-energy SPD were refined based on the Rietveld method. The lattice parameters of 0.7PT-0.3BF were found to be dramatically affected by the particle size [16]. With decreasing particle size, an apparent diminution in the c axis is observed, while the $a(b)$ axis increases slightly. As a result, the unit cell volume (a^2c) is smaller for the smaller particles. It is known that bulk PT-BF perovskite exhibits a great deal of lattice distortion, i.e., tetragonality (c/a). For example, the c/a ratio of PT-BF is as large as 1.18 near the morphotropic phase boundary, which is much greater than that of PT alone (1.064) [17]. PT-BF has the highest c/a in those PT-based perovskites that can be prepared at the atmosphere pressure [18,19]. However, such giant lattice distortion can be easily decreased by reducing the particle size. At a relatively larger particle size (160 nm) for the sample S-II, the c/a ratio decreases from 1.095 of bulk sample S-I to 1.066, resulting in unit cell volume contraction [16]. As a comparison, the lattice parameters of PT begin to be affected at a much smaller size ($\sim$50 nm) [20]. Such size-sensitive property of lattice parameters can be also reflected from the large level on the reduction of the unit cell volume. The volume contraction induced by decreasing the particle size is as high as -2.2% for 0.7PT-0.3BF, which is much larger than that of other materials, such as -0.6% for PT [20], -0.2% for Au [13], and -0.48% for antiperovskite $Mn_3Cu_{0.5}Ge_{0.5}N$ [21]. Since 0.7PT-0.3BF has an unusually strong NTE (CTE: $-2.38 \times 10^{-5}/°C$, RT to 550 °C) [10], such a significant size effect on the unit cell volume is expected to play a strong role in the NTE behavior.

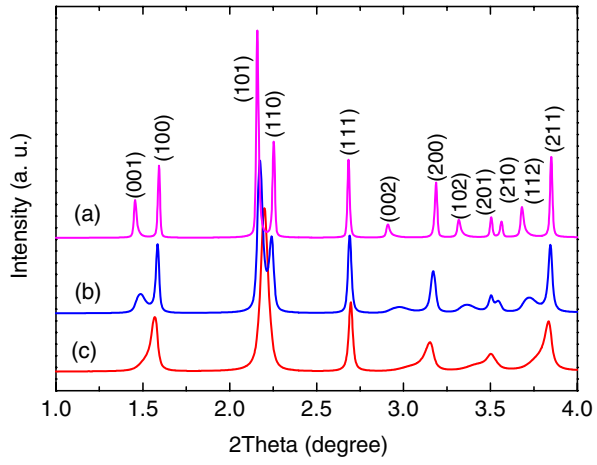

FIG. 1 (color online). High-energy synchrotron powder diffraction patterns of the PT-BF samples S-I (a), S-II (b), and S-IV (c) in a selected short range of 2θ.

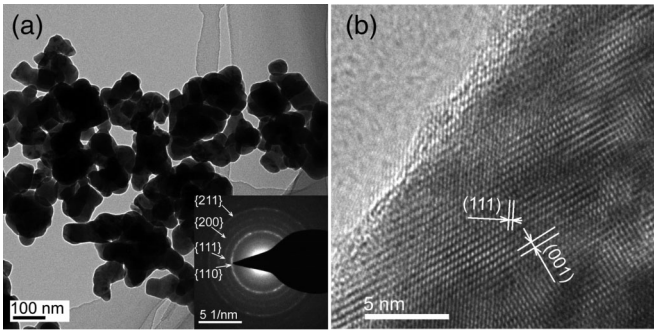

FIG. 2. (a) TEM image with an inset of selected-area electron diffraction. (b) HRTEM image for the PT-BF sample S-IV.

In order to precisely study the thermal expansion, the temperature dependence of the unit cell volume was studied on samples S-II, S-III, and S-IV by means of high-energy SPD (Fig. 3). As the particle size decreases from the bulk state to 160 nm (S-II), the NTE is considerably weakened (CTE: $-0.92 \times 10^{-5}/°C$). As a comparison, the CTE is $-2.38 \times 10^{-5}/°C$ for the bulk state of 0.7PT-0.3BF [11]. However, with further decreases in particle size, a striking change takes place in the thermal expansion of the S-III and S-IV. The unit cell volume of the S-III almost neither contracts nor expands in the ferroelectric phase below its T_C, which could be regarded as ZTE. Here its CTE is as low as $-0.46 \times 10^{-5}/°C$. For the S-IV, the NTE disappears and abnormally transforms into the PTE (CTE: $0.96 \times 10^{-5}/°C$). The transformation of strong negative to positive thermal expansion is a new phenomenon that has not been observed in previous studies on NTE materials. As a comparison, the NTE of ZrW_2O_8 hardly changes with reduced particle size [22]. The NTE can be induced in Au nanoparticles and Bi nanowires, whose bulk state behaves as normal thermal expansion [13,23], or the NTE is enhanced in the in-plane lattice from graphite to graphene [14]. Furthermore, it is also interesting to note that the CTE of the present 0.7PT-0.3BF samples varies in a very large content from -2.38 to $0.96 \times 10^{-5}/°C$, which covers almost all NTE oxides [2]. What accounts for such striking transformation of thermal expansion property? The understanding of this transformation will benefit the control and design of NTE materials.

It should be noted that there is only a slight decrease in the particle size for the 0.7PT-0.3BF. As shown in Fig. 3, the size effect produces a significant impact on the unit cell volume below T_C such as at RT, however, not at temperatures above T_C. The T_C is 540, 520, and 500 °C for the samples S-II, S-III, and S-IV, respectively. The similar unit cell volume of samples S-II, S-III, and S-IV above T_C can be directly supported from the same position of diffraction peak, such as the (200) singlet profile at 540 °C (inset of Fig. 3). In the paraelectric phase above T_C, it is not a surprise to observe a similar unit cell volume, because the perovskite of 0.7PT-0.3BF is in a cubic phase with a close-packed structure, and the unit cell volume is actually determined by the radius of atoms. On the other hand, at RT the unit cell volume is much different, which mainly gives rise to the transformation from the negative to the positive thermal expansion. A smaller unit cell volume at RT means more weakened NTE, such as for the S-II. If the unit cell volume at RT is smaller than the one at T_C, PTE happens, such as for the S-IV. In order to explain such abnormal phenomenon of thermal expansion, we carried out the structural refinements by means of high-energy SPD. The size effect on structural refinement is considered by adopting a two-phase model with two tetragonal components that can give the best refinement, where the major tetragonal component responds to the bulk core phase and the minor one to the less distorted surface layer and domain wall region [24]. For detailed refinement, see the Supplemental Material [16]. The present two-phase model is similar to the composite structure model that was utilized for the refinement of $BaTiO_3$ nanopowders [25,26]. Furthermore, lattice dynamics was also investigated for the polarization property by Raman spectroscopy for the PT-BF samples.

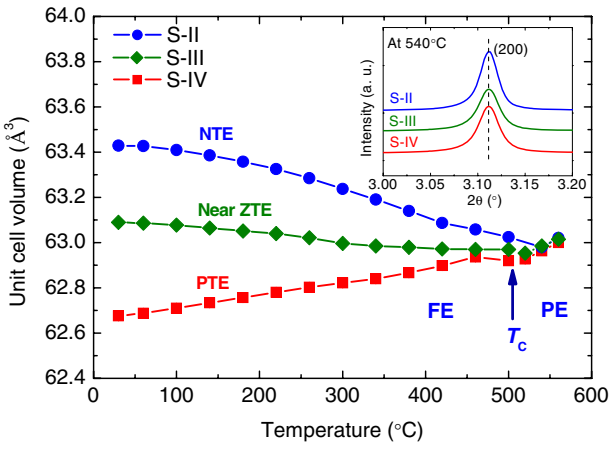

FIG. 3 (color online). Temperature dependence of the unit cell volume of the PT-BF samples. The inset pattern is the singlet profile (200) of cubic phase at 540 °C. FE and PE mean ferroelectric and paraelectric, respectively. The error bars are smaller than symbol size.

For the ferroelectric state, the spontaneous polarization (P_S), formed by dipoles in perovskite lattice, plays an important role in the crystal structure and ferroelectric property [27]. For the bulk sample of 0.7PT-0.3BF (S-I), there is a large P_S displacement at both A and B sites (Supplemental Material Table SI [16]). The A-site P_S displacement (δz_A) is defined as the shift between Pb/Bi cations and centroid of oxygen polyhedron, and the B-site P_S displacement (δz_B) is the shift in the Ti/Fe-O_6 octahedron. The present result of bulk 0.7PT-0.3BF is also in a good agreement with the previous studies by neutron powder diffraction [11]. However, for samples S-II, S-III, and S-IV with a smaller particle size, the P_S displacements are gradually reduced and cannot be maintained at a high level anymore (Supplemental Material Table SI [16]). For example, the A-site P_S displacement (δz_A) descends from 0.5905 Å of the bulk sample S-I to 0.5127 Å of the sample S-IV. It means that the ferroelectricity is weakened in the samples of S-II, S-III, and S-IV. The decrease in the P_S displacement indicates the weakened covalent bonding between cations and oxygen, which is also supported by the elongation in the Pb/Bi-O_2 bond (Supplemental Material Table SI [16]). Therefore, the ferroelectric polar ordering is suppressed in the samples of S-II, S-III, and S-IV. This kind of size effect is also true for other polar compounds, such as ferroelectric $BaTiO_3$, antiferroelectric

$PbZrO_3$, and superconductor $La_{1.85}Sr_{0.15}CuO_4$ [28,29]. With decreasing size, the lattice distortion of these polar compounds gradually transforms into a nonpolar cubic phase [28].

Figure 4 represents the lattice parameters of 0.7PT-0.3BF as function of δz_A for all samples at RT. With decreasing δz_A, i.e., weakening ferroelectricity, the $a(b)$ axis is slightly elongated, while the c axis is rapidly shortened. It can be clearly seen that there is a strong correlation between lattice parameters and ferroelectricity. As a ferroelectricity, the polar directions of A and B sites P_S are aligned parallel along the c axis in the 0.7PT-0.3BF perovskite. The large value of the c axis is originated from the high P_S [27]. However, as the P_S reduces, the c axis shrinks quickly. As a result, the unit cell volume is decreased and dominated by the contribution from the c axis. Here, the sample S-IV has the smallest unit cell volume with weakened ferroelectricity. According to the above results, it is not difficult to understand the unusual transformation behavior of negative to positive thermal expansion. For samples S-I to S-IV, the ferroelectricity is gradually weakened with reducing particle dimension, resulting in a decrease in the unit cell volume at RT. Therefore, the NTE of 0.7PT-0.3BF is correspondingly weakened and finally changes to the PTE.

In order to further confirm the change in the ferroelectricity, a lattice dynamics study was performed by Raman spectroscopy. It has been well studied that ferroelectric soft modes, such as $E(1TO)$ and $A_1(1TO)$, are highly associated with ferroelectric phase transition. Interestingly, the soft mode of $A_1(1TO)$ is sensitive to the P_S, since it represents the opposite vibration between A-site cations with BO_6 octahedra along the P_S direction [30,31]. Previous studies have proved that a strong correlation between $A_1(1TO)$ and P_S is true in systems with not only normally reduced c/a but also enhanced c/a [31]. The soft mode of $A_1(1TO)$ can be used to facilely determine how P_S changes. Figure 5 shows the Raman spectroscopies of PT-BF samples. The individual Raman vibrational modes are calculated by fitting with Lorentz-type profiles. The Raman modes correspond to the space group $P4mm$ [30]. With decreasing particle size, the Raman vibrational modes become broader and broader, which is a common phenomenon in PT ultrafine particles [32]. The soft mode $A_1(1TO)$ of bulk sample S-I is hardened to 173.6 cm^{-1}, when compared with PT (152 cm^{-1}) [31]. The hardening in the $A_1(1TO)$ is well supported by the enhanced P_S displacement. For the samples S-II and S-IV, the $A_1(1TO)$ is softened to lower frequency (170.2 and 166.3 cm^{-1}, respectively), indicating a reduced P_S. Present lattice dynamic observations further support the results demonstrated by the structural refinement.

It is known that ferroelectricity is related to the balance of short-range repulsion favoring cubic phase and long-range Coulomb force favoring ferroelectric order. The equilibrium lattice parameters are dictated by such balance [27]. With decreasing temperature from paraelectric to ferroelectric phase, two factors contribute to the unit cell volume of ferroelectric phase: lattice thermal vibration and ferroelectric order. With decreasing temperature, the contribution from the thermal vibration decreases, and thus the unit cell volume normally contracts. However, the contribution from the ferroelectric order is simultaneously enhanced and makes the unit cell volume oppositely expand. As a result, the volume is a balance between both factors. For all samples of 0.7PT-0.3BF the contribution from the thermal vibration should be the same. However, the contribution from the ferroelectric order is much different. In the bulk sample S-I, the ferroelectric order can be well established, forming a large P_S and increased unit cell volume, and therefore a strong NTE occurs. However, as the particle size decreases, the ferroelectric order is suppressed. Its contribution to the unit cell volume is, therefore, weakened, resulting in a weakened

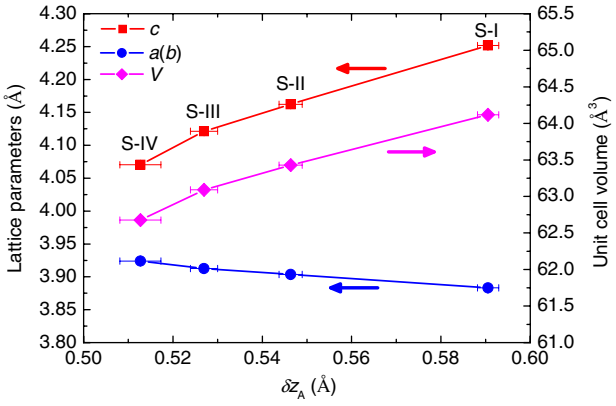

FIG. 4 (color online). Lattice parameters and unit cell volume as function of P_S displacement of δz_A in the PT-BF samples at room temperature.

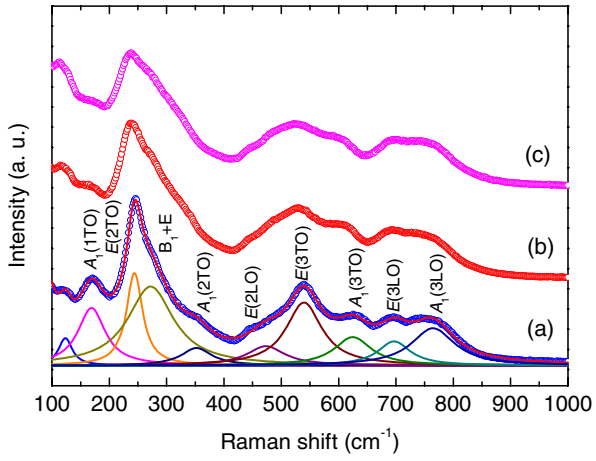

FIG. 5 (color online). Raman spectroscopies of the PT-BF samples, (a) S-I, (b) S-II, and (c) S-IV. The individual vibrational mode is fitted by using a Lorentz profile.

NTE, such as for the sample S-II. As the particle size decreases to a critical value, the contribution of ferroelectric order just matches and counteracts the effect from the lattice thermal expansion. An interesting zero thermal expansion could be achieved. For present studied PT-BF, the critical size is near 140 nm for the sample S-III. The unit cell volume of S-III nearly neither expands nor contracts below its T_C with a small CTE of $-0.46 \times 10^{-5}/°C$ (RT-520 °C). Additionally, it is interesting to observe that the ZTE can persist to high temperature, which is higher than those ZTE materials occurring below RT [21,33]. With further decreasing particle size, the ferroelectric order cannot be well established. Here, the contribution from the ferroelectric order cannot counteract the contribution from the thermal vibration. As a result, PTE appears in the sample S-IV (CTE: $0.96 \times 10^{-5}/°C$).

The present study represents strong evidence for a link between NTE and ferroelectric property. It could be expected that the NTE of ferroelectric materials can be controlled by the adjustment of ferroelectric property. Since there is amount of NTE materials whose NTE is highly correlated with their physical properties, such as magnetism and superconductivity [5,15,21,34], the present study would present a useful way to realize the control of NTE in those functional materials for application in the future.

In summary, PT-BF ferroelectrics with different particle size were prepared by a sol-gel method. The spontaneous polarization is weakened by decreasing particle size investigated by means of synchrotron powder diffraction and Raman spectroscopy. A transformation of strong negative to positive thermal expansion was observed in the PT-BF perovskite, which is highly correlated to the weakening ferroelectricity. A zero thermal expansion is achieved in a wide temperature by adjusting ferroelectric property. The present study presents a new method to control the NTE of functional materials.

This work was supported by the National Natural Science Foundation of China (Grants No. 91022016, No. 21031005, and No. 21231001), the Foundation for the Author of National Excellent Doctoral Dissertation of PR China (201039), Fok Ying Tung Education Foundation (131047), and Program for New Century Excellent Talents in University (NCET-11-0573).

*junchen@ustb.edu.cn
†xing@ustb.edu.cn

[1] T. A. Mary, J. S. O. Evans, T. Vogt, and A. W. Sleight, Science **272**, 90 (1996).
[2] A. W. Sleight, Inorg. Chem. **37**, 2854 (1998).
[3] J. S. O. Evans, J. Chem. Soc. Dalton Trans. 3317 (1999).
[4] W. L. Chen, X. L. Tang, J. A. Muóoz, J. B. Keith, S. J. Tracy, D. L. Abernathy, and B. Fultz, Phys. Rev. Lett. **107**, 195504 (2011).
[5] P. Mohn, Nature (London) **400**, 18 (1999).
[6] Y. W. Long, N. Hayashi, T. Saito, M. Azuma, S. Muranaka, and Y. Shimakawa, Nature (London) **458**, 60 (2009).
[7] J. Chen, X. R. Xing, C. Sun, P. Hu, R. B. Yu, X. W. Wang, and L. H. Li, J. Am. Chem. Soc. **130**, 1144 (2008).
[8] J. Chen, K. Nittala, J. S. Forrester, J. L. Jones, J. X. Deng, R. B. Yu, and X. R. Xing, J. Am. Chem. Soc. **133**, 11114 (2011).
[9] P. Hu, J. Chen, J. X. Deng, and X. R. Xing, J. Am. Chem. Soc. **132**, 1925 (2010).
[10] J. Chen, X. R. Xing, G. R. Liu, J. H. Li, and Y. T. Liu, Appl. Phys. Lett. **89**, 101914 (2006).
[11] J. Chen, X. R. Xing, R. B. Yu, and G. R. Liu, Appl. Phys. Lett. **87**, 231915 (2005).
[12] M. Azuma *et al.*, Nat. Commun. **2**, 347 (2011).
[13] W.-H. Li, S. Y. Wu, C. C. Yang, S. K. Lai, and K. C. Lee, Phys. Rev. Lett. **89**, 135504 (2002).
[14] K. V. Zakharchenko, M. I. Katsnelson, and A. Fasolino, Phys. Rev. Lett. **102**, 046808 (2009).
[15] X. G. Zheng, H. Kubozono, H. Yamada, K. Kato, Y. Ishiwata, and C. N. Xu, Nat. Nanotechnol. **3**, 724 (2008).
[16] See Supplemental Material at http://link.aps.org/supplemental/10.1103/PhysRevLett.110.115901 for details.
[17] V. V. S. S. Sai Sunder, A. Halliyal, and A. M. Umarji, J. Mater. Res. **10**, 1301 (1995).
[18] D. M. Stein, M. R. Suchomel, and P. K. Davies, Appl. Phys. Lett. **89**, 132907 (2006).
[19] M. Yashima, K. Omoto, J. Chen, H. Kato, and X. R. Xing, Chem. Mater. **23**, 3135 (2011).
[20] E. K. Akdogan and A. Safari, J. Appl. Phys. **101**, 064114 (2007).
[21] X. Y. Song, Z. H. Sun, Q. Z. Huang, M. Rettenmayr, X. M. Liu, M. Seyring, G. N. Li, G. H. Rao, and F. X. Yin, Adv. Mater. **23**, 4690 (2011).
[22] P. Badrinarayanan, Md. I. Ahmad, M. Akinc, and M. R. Kessler, Mater. Chem. Phys. **131**, 12 (2011).
[23] L. Li, Y. Zhang, Y. W. Yang, X. H. Huang, G. H. Li, and L. D. Zhang, Appl. Phys. Lett. **87**, 031912 (2005).
[24] H. Boysen, Z. Kristallogr. **220**, 726 (2005).
[25] S. Aoyagi, Y. Kuroiwa, A. Sawada, I. Yamashita, and T. Atake, J. Phys. Soc. Jpn. **71**, 1218 (2002).
[26] S. Aoyagi, Y. Kuroiwa, A. Sawada, H. Kawaji, and T. Atake, J. Therm. Anal. Calorim. **81**, 627 (2005).
[27] R. E. Cohen, Nature (London) **358**, 136 (1992).
[28] S. Tsunekawa, K. Ishikawa, Z.-Q. Li, Y. Kawazoe, and A. Kasuya, Phys. Rev. Lett. **85**, 3440 (2000).
[29] P. Ayyub, V. R. Palkar, S. Chattopadhyay, and M. Multani, Phys. Rev. B **51**, 6135 (1995).
[30] G. Burns and B. A. Scott, Phys. Rev. B **7**, 3088 (1973).
[31] J. Chen, P. Hu, X. Y. Sun, C. Sun, and X. R. Xing, Appl. Phys. Lett. **91**, 171907 (2007).
[32] W. L. Zhong, B. Jiang, P. L. Zhang, J. M. Ma, H. M. Cheng, H. Yang, and L. X. Li, J. Phys. Condens. Matter **5**, 2619 (1993).
[33] S. Margadonna, K. Prassides, and A. N. Fitch, J. Am. Chem. Soc. **126**, 15 390 (2004).
[34] A. C. Mclaughlin, F. Sher, and J. P. Attfield, Nature (London) **436**, 829 (2005).